

6,7-seco-*ent*-Kauranoids Derived from Oridonin as Potential Anticancer Agents

Shengtao Xu,^{†,#} Hong Yao,^{†,#} Mei Hu,[†] Dahong Li,^{†,‡} Zheyang Zhu,[§] Weijia Xie,[†] Hequan Yao,[†] Liang Wu,^{*,†} Zhe-Sheng Chen,[⊥] and Jinyi Xu^{*,†}

[†]State Key Laboratory of Natural Medicines, and Jiangsu Key Laboratory of Drug Screening, China Pharmaceutical University, Nanjing 210009, People's Republic of China

[§]Division of Molecular Therapeutics & Formulation, School of Pharmacy, The University of Nottingham, University Park Campus, Nottingham NG7 2RD, U.K.

[⊥]College of Pharmacy and Health Sciences, St. John's University, Queens, New York, NY 11439, United States

ABSTRACT: Structurally unique 6,7-seco-*ent*-kaurenes, which are widely distributed in the genus *Isodon*, have attracted considerable attention because of their antitumor activities. Previously, a convenient conversion of commercially available oridonin (**1**) to 6,7-seco-*ent*-kaurenes was developed. Herein, several novel spiro-lactone-type *ent*-kaurene derivatives bearing various substituents at the C-1 and C-14 positions were further designed and synthesized from the natural product oridonin. Moreover, a number of seven-membered C-ring expanded 6,7-seco-*ent*-kaurenes were also identified for the first time. It was observed that most of the spiro-lactone-type *ent*-kaurenes tested markedly inhibited the proliferation of cancer cells, with an IC₅₀ value of as low as 0.55 μM. An investigation on its mechanism of action showed that the representative compound **7b** affected the cell cycle and induced apoptosis at a low micromolar level in MCF-7 human breast cancer cells. Furthermore, compound **7b** inhibited liver tumor growth in an in vivo mouse model and exhibited no observable toxic effects. Collectively, the results warrant further preclinical investigations of these spiro-lactone-type *ent*-kaurenes as potential novel anticancer agents.

Nature is an underexplored source of unique and desirable structural scaffolds for novel drug discovery.¹ Many natural products and their derivatives have been developed successfully for clinical applications to treat human diseases in almost all therapeutic areas. Of the 112 first-in-class drugs approved by the U.S. Food and Drug Administration from 1999 to 2013, 31 (28%) were developed based on naturally occurring compounds.²

The genus *Isodon* is well-known for producing bioactive diterpenoids with diverse carbon skeletons.³⁻⁵ More than 700 *ent*-kauranoids have been identified from the genus *Isodon* thus far, including mainly *ent*-kaurenes, 6,7-*seco-ent*-kaurenes, and 8,9-*seco-ent*-kaurenes.⁶ Several *ent*-kaurenes like oridonin (**1**, Scheme 1) and its analogues have been studied extensively for the development of novel anticancer agents.⁷⁻¹¹ Recently, there has been a growing interest in further investigating 6,7-*seco-ent*-kaurene derivatives, which may be classified into the spiro-lactone and enmein-types (Figure 1), because of their broad range of bioactivities.¹²⁻¹⁴ In particular, spiro-lactone-type *ent*-kaurenes bearing diverse chemical skeletons have exhibited promising antitumor activities.^{15,16}

However, for these complex 6,7-*seco-ent*-kaurenes, their isolation from *Isodon* plants in only low yields cannot meet the need for further developmental laboratory studies, while their total synthesis is also quite challenging due to the several stereogenic centers present.¹⁷ In previous work, a convenient conversion of the commercially available oridonin (**1**) to 6,7-*seco-ent*-kaurenes was developed in high yield.¹⁸⁻²⁰ A series of spiro-lactone-type and enmein-type *ent*-kaurenes with diverse chemical properties and potential anticancer activities was synthesized in our laboratory.^{21,22} Among these compounds, several spiro-lactone-type derivatives have been shown to inhibit the proliferation of cancer cells, and some were found to be more potent than their parent compound, oridonin (**1**).²³

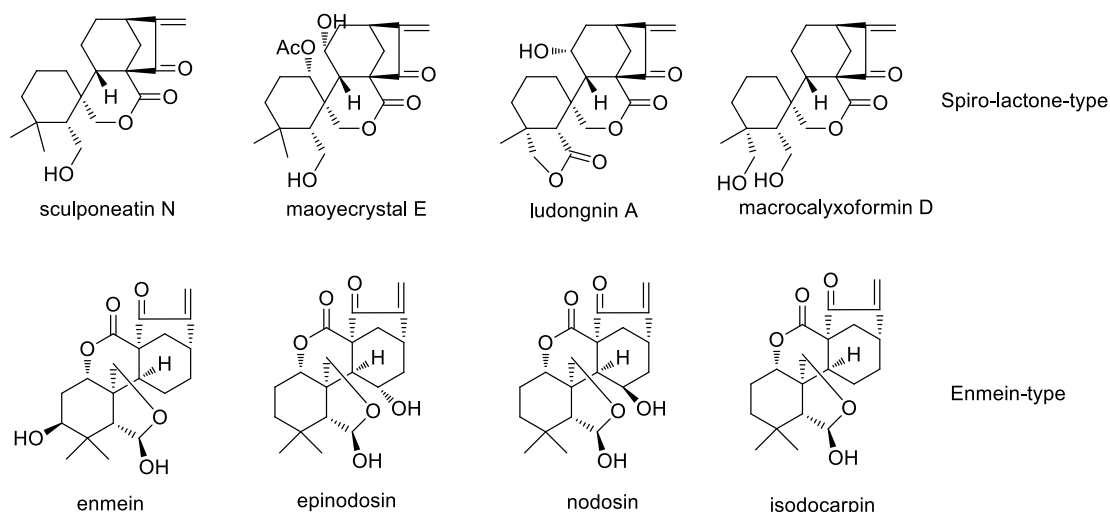


Figure 1. Structures of representative spiro-lactone and enmein-type *ent*-kaurenes isolated from plants.

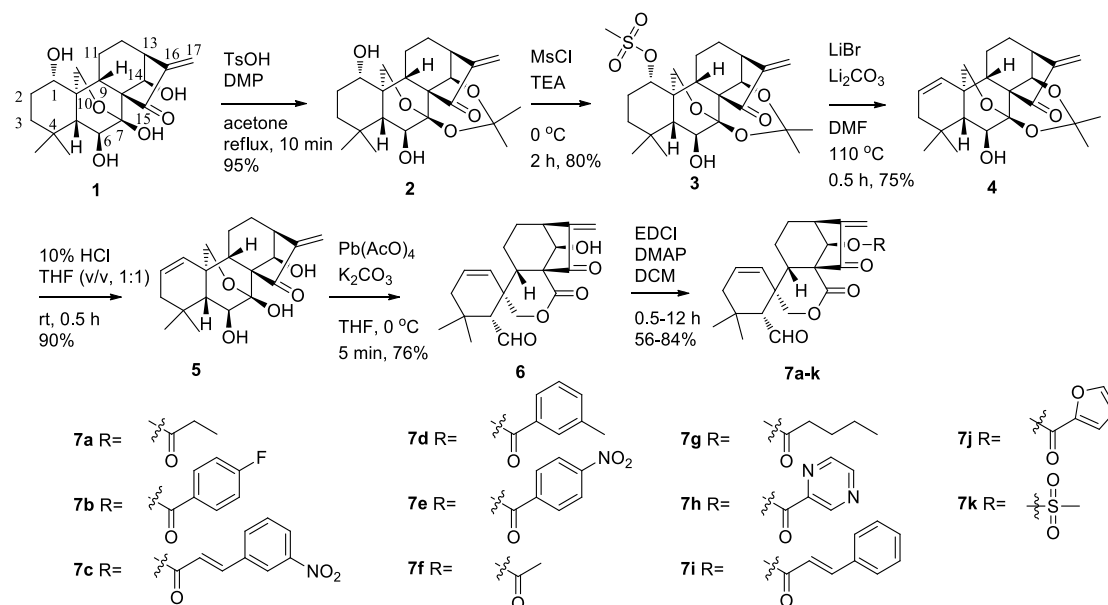
Based on these promising results and the ongoing interest in 6,7-*seco-ent*-kaurenes in the search for anticancer drug candidates with new skeletons, potent antitumor activities, and less toxic effects,^{24,25} several new spiro-lactone-type *ent*-kaurene derivatives bearing various substitutions at the C-1 and C-14 positions have been produced from the commercially available oridonin (**1**), and evaluated for their potential anticancer activities. In addition, the mechanism of action of the representative compound **7b** was investigated in detail.

RESULTS AND DISCUSSION

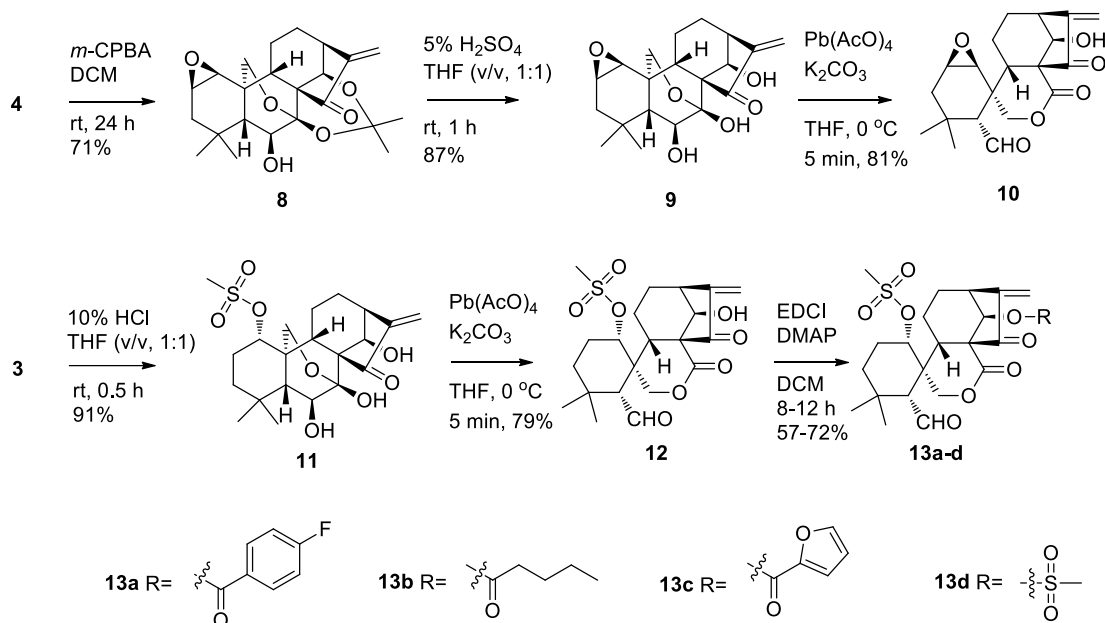
Chemistry. Based on the previous structure-activity relationships (SARs) established,^{26,27} compounds **6**, **10**, and **12** were designed initially by introducing preferred moieties like an alkenyl unit to enhance the resultant activity. The synthesis of the spiro-lactone-type *ent*-kaurenes is outlined in Schemes 1 and 2. Protection of the 7,14-dihydroxy group of oridonin (**1**) with 2,2-dimethoxypropane afforded compound **2** in 95% yield. The 1-hydroxy group of compound **2** was then selectively activated by MsCl, which was eliminated subsequently in the presence of Li₂CO₃ and LiBr in DMF at 110 °C to provide the 1-ene **4** in 75% yield.²⁸ The removal of the acetonide group in the **4** with 10% HCl aqueous solution gave compound **5** in 90%

yield. The conversion of compound **5** to the spiro-lactone-type *ent*-kaurene **6** was achieved successfully by lead tetraacetate oxidation. Compound **6** provided a good building block to construct a library of its 14-*O*-derivatives (**7a-k**) with diverse chemical properties. As shown in Scheme 2, synthon **4** was subjected to epoxidation through *m*-CPBA to give intermediate **8** in 71% yield. The removal of the protecting group with 5% H₂SO₄ provided the desired analogue **9** bearing a C-1,2-epoxy group in 87% yield. The subsequent 6,7-ring opening reaction of compound **9** led to the generation of compound **10** in 81% yield. On the other hand, the removal of the protecting group in **3** with 10% HCl aqueous solution afforded compound **11**, which was further converted to 6,7-*seco*-kaurene **12** using lead tetraacetate in 79% yield. Some derivatives of compound **12** were synthesized by treatment of this substance with various acids in the presence of DMAP and EDCI.

Scheme 1. Synthesis of the 6,7-*seco*-*ent*-Kaurene **6** and Derivatives **7a-k**

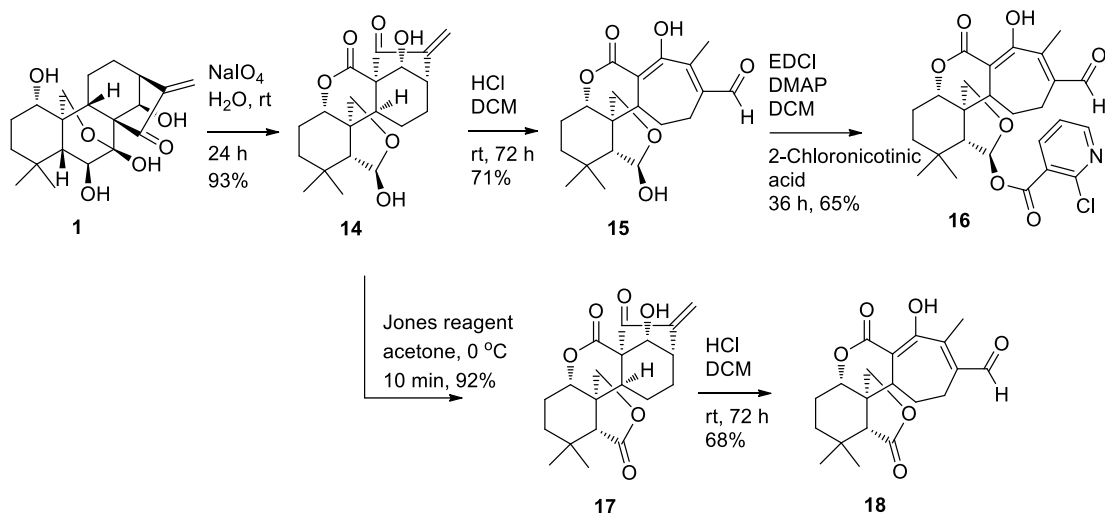


Scheme 2. Synthesis of the 6,7-*seco*-*ent*-Kaurenes **10** and **12** and Derivatives **13a-d**

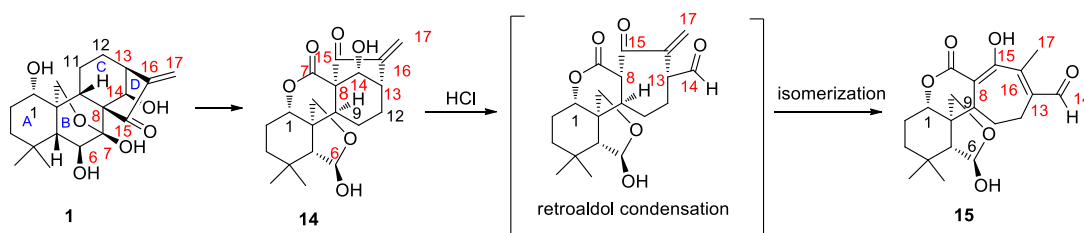


In previous studies, starting from commercially available oridonin (**1**), the enmein-type diterpenoid **14** was obtained by treatment with sodium periodate in water (Scheme 3).¹⁸ Further oxidation of **14** with Jones reagent at 0 °C afforded the corresponding ketone **17** in a total yield of 85%. In the present investigation, further treatment of compounds **14** and **17** with 10% HCl provided the new seven-membered C-ring-expanded analogues **15** and **18**, respectively. A possible mechanism for the formation of these ring-expanded analogues is acid-catalyzed retroaldol condensation and subsequent isomerization to adopt a more stable structure (Scheme 4). The unique skeleton of compound **15**, which contains a seven-membered ring, was identified using 2D-NMR spectroscopy. This type of diterpenoid, bearing a seven-membered ring is rare in Nature, and it may be worthy of further extensive biological evaluation.

Scheme 3. Synthesis of the C-Ring-expanded Kaurenes **15**, **16**, and **18**



Scheme 4. Mechanism of Conversion from Oridonin (**1**) to the C-Ring-expanded *ent*-Kaurene **15**



Structural Identification. During the 1970s and the early 1980s, it was difficult to discriminate between the enmein-type and spiro-lactone-type *ent*-kaurenes due to the lack of sufficiently sensitive NMR spectroscopic methods. For this reason, some spiro-lactone-type compounds were misidentified as enmein-type compounds. In the present study, the structure of the spiro-lactone-type compound **6** was established unambiguously from its 2D NMR spectra. Its molecular formula was determined to be $C_{20}H_{24}O_5$, with nine indices of hydrogen deficiency by HRESIMS ($[M+Na]^+$, 367.1520). The 1H NMR spectrum showed the presence of a formyl group proton doublet (δ_H 9.85, 1H, d, $J = 4.65$ Hz), two exocyclic methylenes (δ_H 6.22 and δ_H 5.62) and two oxygen-bearing methylenes (δ_H 4.35 and δ_H 4.74). The ^{13}C NMR spectrum showed the presence of 20 carbon resonances that were classified as six quaternary carbons, seven methines, five methylenes, and two methyl groups (Table S1, Supporting Information). The key HMBC cross-peaks of H-6 (δ_H 9.85) with C-5 (δ_C

58.7) indicated the attachment of the $-CHO$ moiety at C-5. Moreover, the linkage between C-7 and C-20 via a lactone was supported by the HMBC cross-peaks of H₂-20 (δ_H 4.35 and δ_H 4.74) with C-7 (δ_C 172.8) (Figure 2). Consequently, after careful comparison of the 1H and ^{13}C NMR data of compounds **5** and **6**, compound **6** was assigned structurally as *ent*-6,7,15-trioxo-7,20-epoxy-14 β -hydroxy-1-alkene-6,7-seco-16-kaurene.

The structure of the enmein-type diterpenoid **14** was determined in a previous study,¹⁹ and the gross structure of **15** was elucidated by the analysis of 2D NMR data and by comparison with the NMR data of **14**. The 1H NMR spectrum of **15** exhibited three singlets at δ_H 0.96, 1.05 and 2.34 (Table S2, Supporting Information). After comparison with the NMR data of **14** and **15**, a singlet signal at δ_H 2.34 (3H, s) was attributed to the methyl group at the C-ring, which was isomerized from an exocyclic methylene. Additionally, a deshielded singlet (δ_H 13.99, 1H, s) was observed, and this was attributed to a stable enol due to the presence of an adjacent lactone system. In the HMBC spectrum, a series of key correlations were observed clearly to support the proposed structure: H-14 with C-12 and 13, H-17 with C-13, and OH-15 with C-8 and 16 (Figure 2).

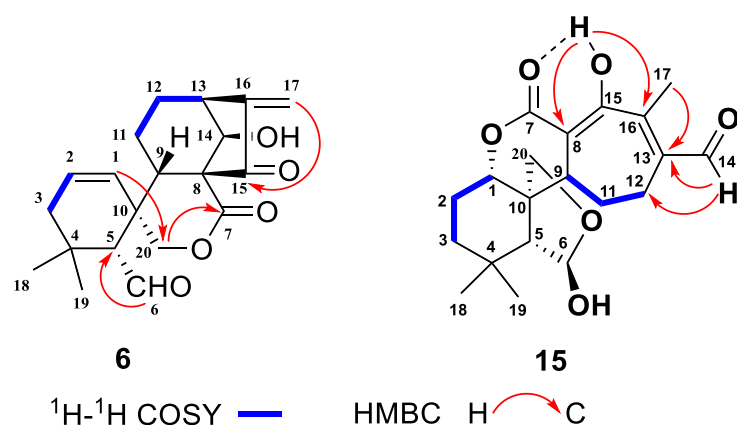


Figure 2. Key 1H - 1H COSY and HMBC correlations of compounds **6** and **15**.

Antiproliferative Effects on Human Cancer Cells. The *in vitro* antiproliferative activities of representative 6,7-seco-*ent*-kaurenes were screened with human

hepatocellular carcinoma Bel-7402 cells using the MTT method (Figure S1, Supporting Information). The results showed that the newly synthesized spiro-lactone-type *ent*-kaurenes (**6**, **10**, and **12**) displayed antiproliferative activities. However, the ring-expanded compounds **15**, **16**, and **18** exhibited much weaker activities against Bel-7402 cells. These results inspired us to further evaluate the detailed antiproliferative activities of spiro-lactone-type kaurenes. As shown in Table 1, although compound **6** in bearing a C-1,2-ene group possessed better cytotoxic potencies against these four types of cancer cells than its parent, oridonin (**1**), the introduction of an epoxy or a mesyl group into the A-ring of these diterpenoids (**10** and **12**) caused a slight decrease in antiproliferative activities relative to **1**. In previous studies, it was found that C-14 oxygenated derivatives of *ent*-kaurenes showed excellent cytotoxicities against human cancer cell lines.²⁹ Therefore derivatives **7a-k** and **13a-d** were further synthesized and evaluated. Interestingly, most of these new C-14 oxygenated derivatives exhibited more potent cytotoxicities than their parent compounds (**6** and **12**), especially against Bel-7402 cells, with IC₅₀ values that varied from 0.57 to 7.1 μM.

Table 1. Antiproliferative Effects of 6,7-*seco-ent*-Kaurenes against Four Human Cancer Cell Lines^a

compound	IC ₅₀ (μM) ^b			
	MGC-803	Bel-7402	MCF-7	K562
1	4.5±0.53	>10.0	9.1±0.86	5.1±0.62
6	3.0±0.19	2.5±0.31	6.4±0.48	4.2±0.58
7a	7.3±0.89	7.1±0.72	3.4±0.38	1.2±0.15
7b	2.2±0.28	1.8±0.19	0.68±0.08	0.69±0.03
7c	2.9±0.28	5.1±0.51	2.2±0.15	1.4±0.18
7d	2.4±0.15	3.6±0.25	1.1±0.09	0.55±0.04
7e	7.3±0.63	>10.0	6.4±0.89	1.0±0.08
7f	0.95±0.07	0.57±0.07	1.0±0.07	0.63±0.03

7g	4.3±0.32	2.2±0.17	3.3±0.21	5.5±0.62
7h	2.8±0.12	1.3±0.10	3.5±0.36	2.9±0.32
7i	0.95±0.05	1.5±0.09	1.5±0.11	1.3±0.10
7j	1.3±0.06	0.84±0.06	1.2±0.17	0.78±0.06
7k	2.8±0.11	1.3±0.23	2.0±0.18	1.9±0.20
10	>10.0	4.6±0.39	>10.0	>10.0
11	3.9±0.43	2.7±0.13	3.9±0.28	3.2±0.32
12	>10.0	>10.0	>10.0	>10.0
13a	4.5±0.54	3.1±0.22	5.5±0.72	6.2±0.43
13b	3.2±0.21	2.2±0.16	3.7±0.21	4.5±0.32
13c	3.4±0.23	1.1±0.12	2.9±0.42	1.7±0.23
13d	8.8±0.68	3.8±0.23	9.5±0.12	1.2±0.15

^aMGC-803, human gastric cancer cells; Bel-7402, human hepatocellular carcinoma cells; MCF-7, human breast cancer cells; K562, human leukemia cells. ^bMTT method, with the cells incubated with the test compounds for 72 h (means ± SD, *n* = 3).

Antiproliferative Effects on Multidrug Resistant Cancer Cells. Multidrug resistance (MDR) is one of the major reasons for the failure of cancer chemotherapy.³⁰ To investigate whether these 6,7-*seco-ent*-kaurenes are effective against drug-resistant cancer cells, the representative derivatives **6** and **7b** were selected to test their antiproliferative activities against drug-resistant and drug-sensitive parental cells, using the MTT method. The results showed that the antiproliferative activities of these synthesized compounds were more potent for the drug-resistant cells (KB/CP4; cisplatin resistant human cervix carcinoma) than for the KB-3-1 paired drug-sensitive cells (Table S3, Supporting Information).

Mechanism of Action Study of Compound 7b. The long-term antiproliferative ability of compound **7b** was demonstrated initially after performing a colony formation assay (Figure S2, Supporting Information).³¹ To determine whether the suppression of cell growth by **7b** is caused by a cell-cycle effect, the DNA content of the cell nuclei was detected by flow cytometry. As seen in Figure 3a, the cells accumulated at the G2/M phase and increased from 12.72% to 24.80% in a dose-dependent manner, with the percentages of cells in the S and G1 phases decreasing concomitantly. The above results suggested that **7b** may inhibit cancer cell proliferation through cell cycle arrest at the G2/M phase.

When MCF-7 and Bel-7402 cells were treated with compounds **6** and **7b** for 24 h, lactate dehydrogenase (LDH) release into the culture medium was not observed (Figure S3, Supporting Information), suggesting that the inhibition of cell viability by these spiro-lactone-type diterpenoids was not by cytotoxicity, but most likely due to cell apoptosis.³² Thus, vehicle or **7b**-treated MCF-7 cells were stained with Annexin V and propidium iodide (PI) followed by flow cytometric analysis. As shown in Figure 3c, treatment with different concentrations of **7b** (0, 0.25, 0.5, 1.0, and 2.0 μ M) resulted in increased amounts of total apoptotic cells in a dose-dependent manner from 2.1% up to 38.7%.

Mitochondria play an essential role in the process of apoptosis.³³ The fluorescent probe JC-1 was used to measure the mitochondrial membrane potential (MMP) after the treatment of **7b**. The results showed that **7b** treatment in MCF-7 cells induced the dissipation of MMP in a dose-dependent manner, as indicated by a decrease in red fluorescence emission and an increase in green fluorescence emission (Figure S4, Supporting Information).

Finally, Western blotting analysis was performed to evaluate the expression of apoptosis-related proteins.³⁴ As shown in Figure 4, the results revealed that incubation with compound **7b** dramatically increased the relative levels of Bax, caspase 3, p-ERK, and reduced the levels of Bcl-2 and P53 expression in a concentration-dependent manner.

Taken together, these results demonstrated that **7b** induced apoptosis in MCF-7

cancer cells through a mitochondria-related apoptotic pathway.

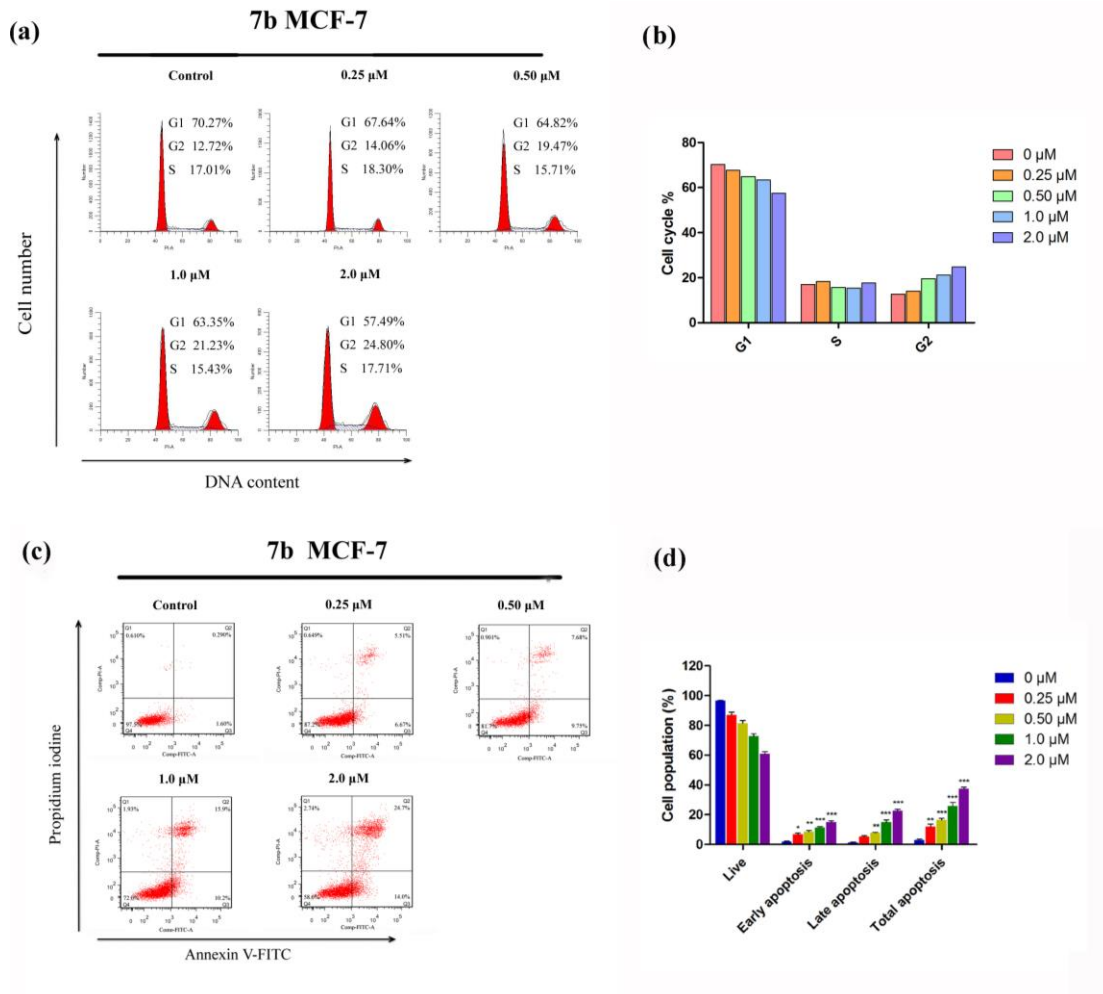


Figure 3. Compound **7b** caused G2/M arrest and apoptosis of MCF-7 cancer cells. (a) MCF-7 cells were treated with DMSO and varying concentrations of **7b** (0.25, 0.5, 1.0, and 2.0 μM) for 48 h, then cells were harvested, stained with PI, and analyzed by flow cytometry; (b) Histograms displaying the percentage of cell cycle distribution; (c) MCF-7 cells were treated with varying concentrations of **7b** (0.25, 0.5, 1.0, and 2.0 μM). After 24 h of treatment, cells were collected and stained with Annexin V/PI, followed by flow cytometric analysis; (d) Histograms displaying the percentage of cell distribution. Data are represented as means \pm SD of three independent experiments (* $p < 0.05$, ** $p < 0.01$, and *** $p < 0.001$ vs. control group).

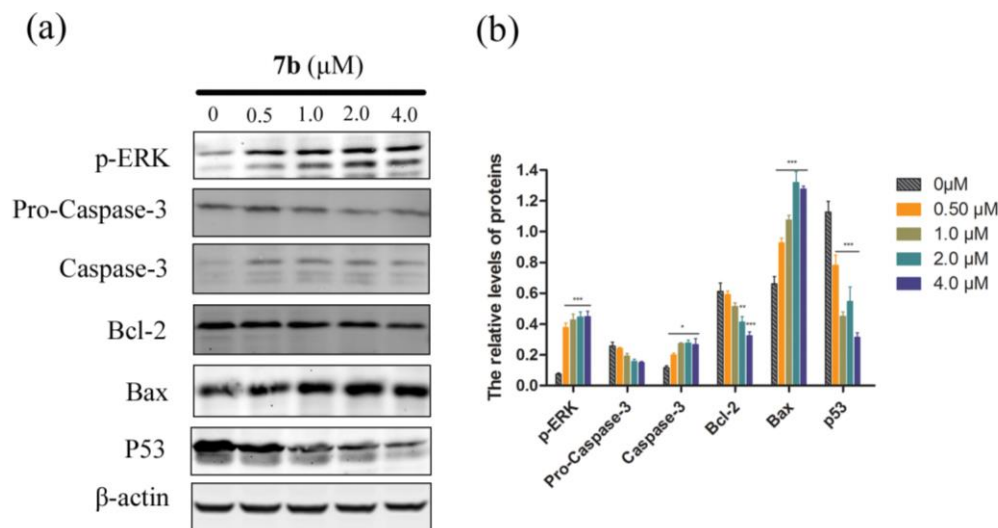


Figure 4. MCF-7 cells were treated with various concentrations of **7b** (0, 0.5, 1.0, 2.0, and 4.0 μM) for 48 h. (a) The expression of p-ERK, pro-caspase-3, caspase-3, bcl-2, bax, and p53 was determined by Western blotting using specific antibodies. β -Actin was used as internal control; (b) The density ratio of proteins to β -actin is shown as relative expression. Data are represented as means \pm SD of three independent experiments (* p < 0.05, ** p < 0.01, *** p < 0.001; control compared with **7b**-treated cells).

In Vivo Antitumor Activity of Compound 7b. To evaluate the in vivo antitumor activity of compound **7b**, groups of mice were treated with 10 or 20 mg/kg of compound **7b** or 20 mg/kg of oridonin (**1**) once a day, respectively. As shown in Figures 5a and 5b, treatment with 20 mg/kg of **7b** enhanced the inhibitory effect on the tumor volume with an inhibition rate of 52.5%, which was equivalent to that of oridonin (**1**) (51.2%). When the mice were sacrificed at the end of the observation, the tumors were excised and weighed. The results also showed statistically significant reductions in tumor weight in both doses of the **7b**-treated mice (Figure 5c). Moreover, there was no significant weight loss in mice treated with **7b** when compared with those in the vehicle control group (Figure 5d). Taken together, these data indicated that compound **7b** was efficacious in inhibiting the growth of liver cancer growth in vivo and may be worthy of further evaluation.

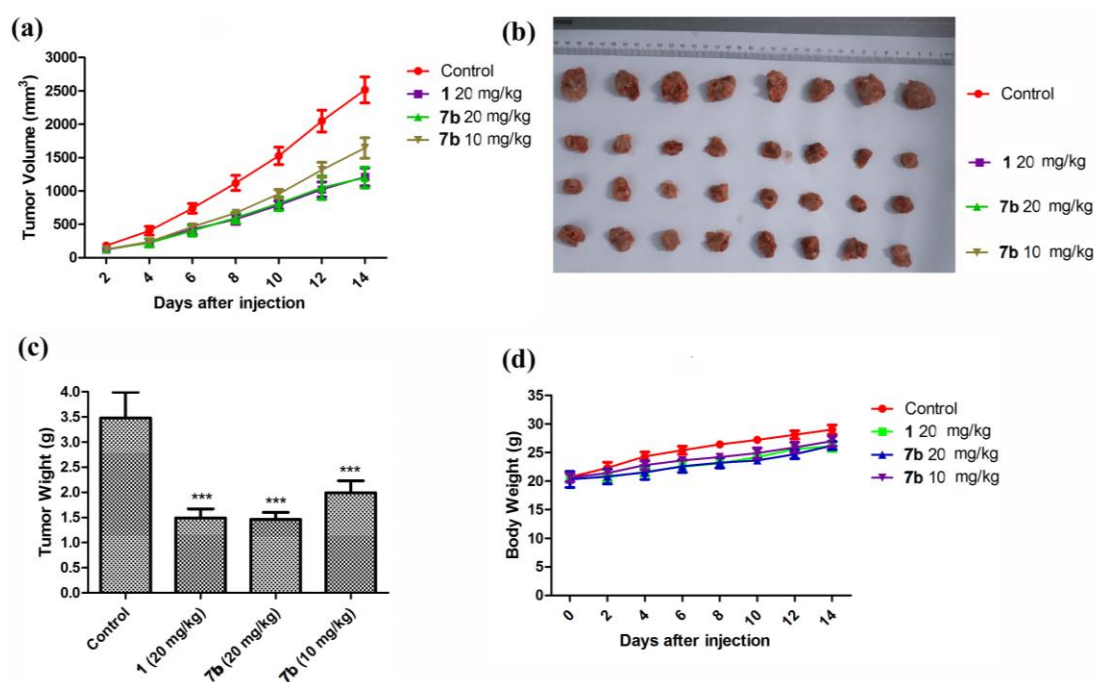


Figure 5. Compound **7b** exhibited antitumor activity in vivo. (a) H22 cells were inoculated subcutaneously into the right flank of mice. The mice were divided randomly into four groups ($n = 8$) and treated intravenously with **7b** (20 mg/kg and 10 mg/kg), oridonin (**1**, 20 mg/kg), and DMSO (dissolved in sodium chloride, control) each day for two weeks; (b) Visible tumor formation and photographs of tumors removed from mice at 14 days after initiation of treatment; (c) Treatment with **7b** resulted in significant lower tumor weight compared with controls ($***p < 0.001$); (d) Body weight changes of mice during treatment.

In summary, several new spiro-lactone-type *ent*-kaurene derivatives with potent antiproliferative activities were synthesized from the commercially available diterpenoid oridonin (**1**). Furthermore, several C-ring expanded 6,7-*seco-ent*-kaurenes, each bearing a seven-membered ring, were also produced. The in vitro antiproliferative results showed that all the spiro-lactone-type 6,7-*seco-ent*-kaurenes inhibited the proliferation of cancer cells, but the seven-membered C-ring expanded 6,7-*seco-ent*-kaurenes (**15**, **16**, and **18**) were inactive. It was found that the representative compound **7b** caused cell-cycle arrest and induced apoptosis in MCF-7

cells through a mitochondria-related apoptotic pathway, and the antitumor activity of compound **7b** was verified in a liver cancer xenograft mouse model with no observable toxicity.

EXPERIMENTAL SECTION

General Experimental Procedures. Oridonin (**1**) was purchased from Nanjing Zelang Chemical Co., Ltd. (Zelang, People's Republic of China) with a stated purity of 98%. All commercially available reagents were used without further purification. Anhydrous solvents were dried through routine protocols. ¹H NMR and ¹³C NMR spectra were recorded with a Bruker AV-300 spectrometer (Bruker Company, Germany) in the indicated solvents (CDCl₃ or DMSO-*d*₆, TMS as internal standard); the values of the chemical shifts are expressed in δ values (ppm) and the coupling constants (*J*) in Hz. Low- and high-resolution mass spectrometry (ESIMS and HRESIMS) were measured on a Finnigan MAT 95 spectrometer (Finnigan, Germany). Flash column chromatography was carried out on 200-300 mesh silica gel purchased from Qingdao Haiyang Chemical Co., Ltd. (Qingdao, People's Republic of China). Reactions were monitored by thin-layer chromatography (TLC) on 0.25 mm silica gel plates (GF₂₅₄) and visualized under UV light.

The general procedure for the synthesis of compounds **2-18** is provided in the Supporting Information, where full details of their purification and spectroscopic data are provided. Such information is given for compound **7b** (testing biologically and mechanistically) below.

ent-6,7,15-Trioxo-7,20-epoxy-(14 β -O-p-flourobenzoyl)-1-alkene-6,7-seco-16-kaurene (7b). Compound **6** (72 mg, 0.2 mmol) was dissolved in dichloromethane, then EDCI, DMAP, and parafluorobenzoic acid (34 mg, 0.24 mmol) were added. The reaction mixture was stirred at room temperature for about 2 h. Then the mixture was washed with 10% HCl. The organic layer was washed with brine and dried over anhydrous Na₂SO₄. After flash chromatography (MeOH-CH₂Cl₂ 1: 300, v/v), compound **7b** was obtained as a white solid (48 mg, 69%): ¹H NMR (CDCl₃, 300 MHz) δ 9.91 (1H, d, *J* = 5.7 Hz), 7.85 (2H, m), 6.98 (2H, t, *J* = 8.4 Hz), 6.21 (1H, s),

5.99 (1H, m), 5.67 (2H, m), 5.47 (1H, s), 4.85, 4.60 (each 1H, dd, $J_A = J_B = 10.8$ Hz), 3.32 (1H, s), 2.27 (1H, m), 2.21 (1H, m), 1.97 (1H, d, $J = 5.7$ Hz), 1.88 (3H, m), 1.59 (3H, m), 1.18 (3H, s), 0.91 (3H, s); ^{13}C NMR (CDCl_3 , 75 MHz) δ 203.6, 197.4, 167.8, 144.5, 132.9, 132.8, 132.6, 132.5, 131.7, 126.6, 119.6, 115.6, 75.7, 67.4, 62.9, 61.1, 45.5, 43.5, 43.2, 40.1, 32.5, 31.2, 30.1, 22.5, 17.8; ESIMS m/z 467.2 $[\text{M}+\text{H}]^+$; HRESIMS m/z 489.1682 $[\text{M}+\text{Na}]^+$ (calcd for $\text{C}_{27}\text{H}_{27}\text{NaFO}_6$ 489.1684).

Cytotoxicity Determination. The inhibitory effect of compounds on human cancer cell growth was determined using a colorimetric MTT assay. Briefly, the cell lines (MGC-803, Bel-7402, MCF-7, and K562; purchased from ATCC) were incubated at 37 °C in a humidified 5% CO_2 incubator for 24 h in 96-microwell plates prior to the experiments. After medium removal, 100 μL of fresh medium containing the test compound at different concentrations were added to each well and incubated at 37 °C for 48 or 72 h. The percentage of DMSO in the medium did not exceed by 0.25%. The number of living cells after 72 h (or 48 h) of culture in the presence (or absence: control) of the various compounds was directly proportional to the intensity of the purple color generated, which was measured quantitatively by spectrophotometry at a 570 nm wavelength. The experiment was performed in quadruplicate and repeated three times.

Colony Formation Assay. Initially, 300 MCF-7 cells were plated per well in 30 mm plates. After an overnight incubation, the cells were treated with various concentrations of **7b** dissolved in DMSO. As a negative control, some cells were treated with vehicle (DMSO) only. After 24 h, the medium was removed and cells were allowed to grow for ten days. Subsequently, the cells were fixed with methanol for 15 min and stained with 0.1% crystal violet for 15 min. After removing the crystal violet by washing, the plates were photographed and counted, with one colony defined to be an aggregate of >50 cells. At least three independent experiments were performed for each assay.

Cell Cycle Analysis. Altogether, 5×10^4 cells were seeded into each well of a six-well plate and incubated overnight. Cells then were treated with various concentrations of each test compound for 48 h. The cells were harvested, washed with cold PBS, and then fixed with 70% ethanol in PBS at $-20\text{ }^\circ\text{C}$ for 12 h. Subsequently, the cells were resuspended in PBS containing $100\text{ }\mu\text{g/mL}$ RNase and $50\text{ }\mu\text{g/mL}$ PI and incubated at $37\text{ }^\circ\text{C}$ for 30 min. Cell cycle distribution of nuclear DNA was determined by flow cytometry on an FC500 cytometer (Beckman Coulter).

Cell Cytotoxicity. To measure cell cytotoxicity, MCF-7 and Bel-7402 cells were seeded at a density of $\sim 5 \times 10^3$ cells per well in 96-well plates for 24 h, followed by incubation with the test compounds for 36 h. Then, the medium was collected and measured for cytotoxicity (LDH assay Kit; Promega), according to a standard protocol. The assay plate was allowed to equilibrate to ambient temperature, and CytoTox-ONETM reagent was added to each well and incubated for 10 min. Next, a stop solution was added, and the fluorescent signal was measured with an excitation wavelength of 560 nm and an emission wavelength of 590 nm.

JC-1 Assay to Determine Mitochondrial Membrane Potential (MMP). The MMP was determined using the dual-emission mitochondrial dye JC-1. After treatment with various concentrations of **7b** for 36 h, MCF-7 cells were loaded with $10\text{ }\mu\text{g/mL}$ JC-1 dye for 30 min at $37\text{ }^\circ\text{C}$ and then washed for 5 min in PBS buffer. After incubation, samples were immediately assessed for red and green fluorescence with a microplate reader or using fluorescence microscopy. The fluorescent signal of the monomers was measured at an excitation wavelength of 490 nm and an emission wavelength of 535 nm. The fluorescent signal of aggregates was detected with an excitation wavelength of 525 nm and an emission wavelength of 600 nm. All experiments were performed in triplicate.

Flow Cytometry Analysis of Apoptotic Cells. MCF-7 cells (1×10^5 /well) were cultured in complete medium in six-well plates for 24 h and treated in triplicate with

different concentrations of **7b** for 24 h. The control cells were treated with vehicle (1% DMSO in complete medium). The cells were harvested, washed and stained with propidium iodide (PI), and FITC-Annexin V in the dark for 15 min using the FITC-AnnexinV Kit (BD Pharmingen, San Diego, CA, USA). The percentages of apoptotic cells were determined by flow cytometry on an FC500 cytometer (Beckman Coulter).

Western Blotting Analysis. MCF-7 cells were incubated in the presence of **7b** and collected after 48 h. Cells were centrifuged and washed two times with ice-cold phosphate buffered saline. The pellet was then resuspended in lysis buffer. After the cells were lysed on ice for 20 min, lysates were centrifuged at 13,000 g at 4 °C for 15 min. The protein concentration in the supernatant was determined using the BCA protein assay reagent. Equal amounts of protein (20 μ g) were resolved using sodium dodecyl sulfate-polyacrylamide gel electrophoresis (SDS-PAGE) (8-12% acrylamide gel) and transferred to PVDF Hybond-P membrane. Membranes were blocked for 1 h at room temperature. Membranes were then incubated with primary antibodies against caspase-3, pro-caspase-3, Bax, Bcl-2, p-ERK, P53, β -actin, with gentle rotation overnight at 4 °C. Membranes were next incubated with fluorescent secondary antibodies for 60 min.

In Vivo Tumor Xenograft Study. Five-week-old male Institute for Cancer Research (ICR) mice were purchased from Shanghai SLAC Laboratory Animals Co. Ltd. Altogether, 1×10^6 H22 cells were inoculated subcutaneously into the right flank of ICR mice according to a standard protocol, to initiate tumor growth. After 7 days of tumor transplantation, mice in the H22 group were weighted and divided into four groups of eight animals at random. The groups of **7b** were administered intravenously 10 and 20 mg/kg in a vehicle of 10% DMF/2% poloxamer/88% saline. The positive-control group was treated with oridonin (**1**) (20 mg/kg) through intravenous injection. The negative control group received 0.9% normal saline through intravenous injection. Treatments were done at a frequency of intravenous injection of

one dose per day for a total 14 consecutive days. Body weights and tumor volumes were measured every two days. After the treatments, all of the mice were sacrificed and weighed. The following formula was used to determine tumor volumes: tumor volume = $L \times W^2/2$, where L is the length and W the width. Ratio of inhibition of tumor (%) = $(1 - \text{average tumor weight of treated group}/\text{average tumor weight of control group}) \times 100\%$. All procedures were performed in accordance with the *NIH Guide for the Care and Use of Laboratory Animals*. All animal handling and procedures were approved by the Ethical Committee of the China Pharmaceutical University (No. SYXK2016-0011).

Statistics. Statistical analyses were performed using Graphpad Prism (San Diego, CA, USA). The results were expressed as means \pm standard deviations (SD). Student's t -test was employed to determine the statistical differences, and results were considered statistically significant at the level of $*p < 0.05$, $**p < 0.01$, or $***p < 0.0001$.

ASSOCIATED CONTENT

Supporting Information

The Supporting Information is available free of charge on the ACS Publications website at DOI:

AUTHOR INFORMATION

Corresponding Authors

*Tel (L. Wu): +86 025-83271299. Fax: +86 025-83302827. E-mail: wul2004@hotmail.com.

*Tel (J.Y. Xu): +86 025-83271299. Fax: +86 025-83302827. E-mail: jinyixu@china.com.

Notes

[#]These authors contributed equally to this work.

‡Present address: Key Laboratory of Structure-Based Drug Design & Discovery of Ministry of Education and School of Traditional Chinese Materia Medica, Shenyang Pharmaceutical University, Shenyang 110016, People's Republic of China

ACKNOWLEDGMENTS

This work was supported by the National Natural Science Foundation of China (nos. 81373280, 81673306), the Open Project of the State Key Laboratory of Natural Medicines, China Pharmaceutical University (No. SKLNMKF201710), and the China Postdoctoral Science Foundation (No. 2015M581903).

REFERENCES

- (1) Cragg, G. M.; Newman, D. J. *Biochim. Biophys. Acta* **2013**, *1830*, 3670-3695.
- (2) Katz, L.; Baltz, R. H. *J. Ind. Microbiol. Biotechnol.* **2016**, *43*, 155-176.
- (3) Yao, R.; Chen, Z. L.; Zhou, C. C.; Luo, M.; Shi, X. J.; Li, J. G.; Gao, Y. B.; Zhou, F.; Pu, J. X.; Sun, H. D.; He, J. *J. Nat. Prod.* **2015**, *78*, 10-16.
- (4) Yang, J.; Wang, W. G.; Wu, H. Y.; Du, X.; Li, X. N.; Li, Y.; Pu, J. X.; Sun, H. D. *J. Nat. Prod.* **2016**, *79*, 132-140.
- (5) Yang, J.; An, Y. Q.; Wu, H. Y.; Liu, M.; Wang, W. G.; Du, X.; Li, Y.; Pu, J. X.; Sun, H. D. *Sci. China Chem.* **2016**, *59*, 1211-1215.
- (6) Sun, H. D.; Huang, S. X.; Han, Q. B. *Nat. Prod. Rep.* **2006**, *23*, 673-698.
- (7) Ding, C. Y.; Zhang, Y. S.; Chen, H. J.; Yang, Z. D.; Wild, C.; Chu, L. L.; Liu, H. L.; Shen, Q.; Zhou, J. *J. Med. Chem.* **2013**, *56*, 5048-5058.
- (8) Ding, C. Y.; Zhang, Y. S.; Chen, H. J.; Yang, Z. D.; Wild, C.; Ye, N.; Ester, C. D.; Xiong, A. L.; White, M. A.; Shen, Q.; Zhou, J. *J. Med. Chem.* **2013**, *56*, 8814-8825.
- (9) Wu, J.; Ding, Y.; Chen, C. H.; Zhou, Z. M.; Ding, C. Y.; Chen, H. Y.; Zhou, J. Chen, C. S. *Cancer Lett.* **2016**, *380*, 393-402.
- (10) Chen, W.; Zhou, J.; Wu, K.; Huang, J.; Ding, Y.; Yun, E. J.; Wang, B.; Ding, C.; Hernandez, E.; Santoyo, J.; Chen, H.; Lin, H.; Sagalowsky, A.; He, D.; Zhou, J.; Hsieh, J. T. *Oncotarget* **2016**, *7*, 56842-56854.

- (11) Liu, Q. Q.; Wang, H. L.; Chen, K.; Wang, S. B.; Xu, Y.; Ye, Q.; Sun, Y. W. *J. Dig. Dis.* **2016**, *17*, 104-112.
- (12) Lazarski, K. E.; Moritz, B. J.; Thomson, R. J. *Angew. Chem. Int. Ed.* **2014**, *53*, 10588-10599.
- (13) Yeoman, J. T.; Mak, V. W.; Reisman, S. E. *J. Am. Chem. Soc.* **2013**, *135*, 11764-11767.
- (14) Pan, Z. Q.; Zheng, C. Y.; Wang, H. Y.; Chen, Y. H.; Li, Y.; Cheng, B.; Zhai, H. B. *Org. Lett.* **2014**, *16*, 216-219.
- (15) Moritz, B. J.; Mack, D. J.; Tong, L. C.; Thomson, R. J. *Angew. Chem. Int. Ed.* **2014**, *53*, 2988-2991.
- (16) Li, X.; Pu, J. X.; Weng, Z. Y.; Zhao, Y.; Zhao, Y.; Xiao, W. L.; Sun, H. D. *Chem. Biodivers.* **2010**, *7*, 2888-2896.
- (17) Maimone, T. J.; Baran, P. S. *Nat. Chem. Biol.* **2007**, *3*, 396-407.
- (18) Wang, L.; Li, D. H.; Xu, S. T.; Cai, H.; Yao, H. Q.; Zhang, Y. H.; Jiang, J. Y.; Xu, J. Y. *Eur. J. Med. Chem.* **2012**, *52*, 242-250.
- (19) Li, D. H.; Xu, S. T.; Cai, H.; Pei, L. L.; Zhang, Y. H.; Wang, L.; Yao, H. Q.; Wu, X. M.; Jiang, J. Y.; Sun, Y. J.; Xu, J. Y. *Eur. J. Med. Chem.* **2013**, *64*, 215-221.
- (20) Li, D. H.; Xu, S. T.; Cai, H.; Pei, L. L.; Wang, L.; Wu, X. M.; Yao, H. Q.; Jiang, J. Y.; Sun, Y. J.; Xu, J. Y. *ChemMedChem.* **2013**, *8*, 813-818.
- (21) Li, D. H.; Cai, H.; Jiang, B. W.; Liu, G. Y.; Wang, Y. T.; Wang, L.; Yao, H. Q.; Wu, X. M.; Sun, Y. J.; Xu, J. Y. *Eur. J. Med. Chem.* **2013**, *59*, 322-328.
- (22) Li, D. H.; Hu, X.; Tong, T.; Xu, S. T.; Zhou, T. T.; Wang, Z. Z.; Cheng, K. G.; Li, Z. L.; Hua, H. M.; Xiao, W.; Xu, J. Y. *Int. J. Mol. Sci.* **2016**, *17*, E747.
- (23) Ding, Y.; Ding, C. Y.; Ye, N.; Liu, Z. Q.; Wold, E. A.; Chen, H. Y.; Wild, C.; Shen, Q.; Zhou, J. *Eur. J. Med. Chem.* **2016**, *122*, 102-117.
- (24) Li, D. H.; Han, T.; Liao, J.; Hu, X.; Xu, S. T.; Tian, K. T.; Gu, X. K.; Cheng, K. G.; Li, Z. L.; Hua, H. M.; Xu, J. Y. *Int. J. Mol. Sci.* **2016**, *17*, E1395.
- (25) Xu, S. T.; Luo, S. S.; Yao, H.; Cai, H.; Miao, X. M.; Wu, F.; Yang, D. H.; Wu, X. M.; Xie, W. J.; Yao, H. Q.; Chen, Z. S.; Xu, J. Y. *J. Med. Chem.* **2016**, *59*, 5022-5023.
- (26) Bohanon, F. J.; Wang, X. F.; Graham, B. M.; Ding, C. Y.; Ding, Y.;

Radhakrishnan, G. L.; Rastellini, C. R.; Zhou, J.; Radhakrishnan, R. S. *J. Surg. Res.* **2015**, *199*, 441-449.

(27) Xu, S. T.; Yao, H.; Luo, S. S. Zhang, Y. K.; Yang, D. H.; Li, D. H.; Wang, G. Y.; Hu, M.; Qiu, Y. Y.; Wu, X. M.; Yao, H. Q.; Xie, W. J.; Chen, Z. S.; Xu, J. Y. *J. Med. Chem.* **2017**, *60*, 1449-1468.

(28) Ding, C. Y.; Zhang, Y. S.; Chen, H. J.; Wild, C.; Wang, T. Z.; White, M. A.; Shen, Q.; Zhou, J. *Org. Lett.* **2013**, *15*, 3718-3721.

(29) Xu, S. T.; Pei, L. L.; Wang, C. Q.; Zhang, Y. K.; Li, D. H.; Yao, H. Q.; Wu, X. M.; Chen, Z. S.; Sun, Y. J.; Xu, J. Y. *ACS Med. Chem. Lett.* **2014**, *5*, 797-802.

(30) Li, W.; Zhang, H.; Assaraf, Y. G.; Zhao, K.; Xu, X. J.; Xei, J. B.; Yang, D. H.; Chen, Z. S. *Drug Resist. Updat.* **2016**, *27*, 14-29.

(31) Lei, K. F.; Wu, Z. M.; Huang, C. H. *Biosens. Bioelectron.* **2015**, *74*, 878-885.

(32) Bagchi, D.; Bagchi, M.; Hassoun, E. A.; Stohs, S. J. *Toxicology* **1995**, *104*, 129-140.

(33) Jeong, S. Y.; Seol, D. W. *BMB Rep.* **2008**, *41*, 11-22.

(34) Liu, J.; Yao, Y. Z.; Ding, H. F.; Chen, R. A. *Tumour Biol.* **2014**, *35*, 5409-5415.